| | |
|---|---|
| Title: | Shear strength evaluation of RC bridge deck slabs according to CSCT with multi – layered shell elements and PARC_CL Crack Model |
| Authors: | Belletti B., Scolari M., Muttoni A., Cantone R. |
| Published in: | IABSE Conference Geneva 2015 |
| Pages: | pp. 1158-1165 |
| City, country: | Geneva, Switzerland |
| Year of publication: | 2015 |
| Type of publication: | Peer reviewed conference paper |

| | |
|---|---|
| Please quote as: | Belletti B., Scolari M., Muttoni A., Cantone R., *Shear strength evaluation of RC bridge deck slabs according to CSCT with multi – layered shell elements and PARC_CL Crack Model*, IABSE Conference Geneva 2015, Geneva, Switzerland, 2015, pp. 1158-1165. |

# Shear strength evaluation of RC bridge deck slabs according to CSCT with multi – layered shell elements and PARC_CL Crack Model

**Beatrice Belletti, Matteo Scolari**

*Department of Civil Engineering, University of Parma, Parma, Italy*

**Aurelio Muttoni, Raffaele Cantone**

*Ecole Polytechnique Fédérale de Lausanne, Lausanne, Switzerland*

**Contact :** beatrice.belletti@unipr.it

## Abstract

The shear resistance of RC slabs without shear reinforcement subjected to concentrated loads near linear support is usually calibrated on the base of tests on one – way slabs with rectangular cross section. However, the actual behavior of slabs subjected to concentrated loads is described properly by a two-way slab response. The aim of this paper consists in the evaluation of the shear resistance of bridge deck slabs using analytical formulations and Nonlinear Finite Element Analyses (NLFEA). The obtained numerical results are consequently compared with experimental observations from two test campaigns. The case studies were analysed by NLFE analyses carried out using the constitutive Crack Model PARC_CL (Physical Approach for Reinforced Concrete under Cycling Loading) implemented in the user subroutine UMAT.for in Abaqus Code. In order to predict properly global and local failure modes through a NLFE model, a multi – layered shell modelling has been used. As shell element modelling is not able to detect out – of – plane shear failures, the ultimate shear resistance of these slabs is evaluated by means of a post – processing method according to the Critical Shear Crack Theory (CSCT).

**Keywords:** Reinforced Concrete, Deck Slabs, Shear Strength, Nonlinear Finite Elements Analyses

## 1 Introduction

In the past, deck slabs of RC hollow box or T – beam bridges have been designed without shear reinforcement. In many cases, the structural safety cannot be verified by the new Codes for most of them, [1]. Hence, it is necessary to reassess the shear capacity of these bridges: the shear resistance design value $V_{Rd,c}$ of members without shear reinforcement is only based on empirical equations and not on a mechanical model that could take into account of different shear –bearing mechanisms. Linearly supported RC slabs without shear reinforcement subjected to concentrated loads can fail in shear, [2]. Shear can be assessed with two different approaches: by checking the punching shear resistance on a control perimeter around the loading area or by evaluating the beam shear resistance over a prescribed effective width $b_w$, [3] - [5], (Figure 1). The load carrying mechanisms for linearly supported RC slabs under concentrated loads is different for one –way or two – way slabs as the acting shear forces and bending moments at the shear critical region could potentially vary by increasing the level of load due to redistribution of

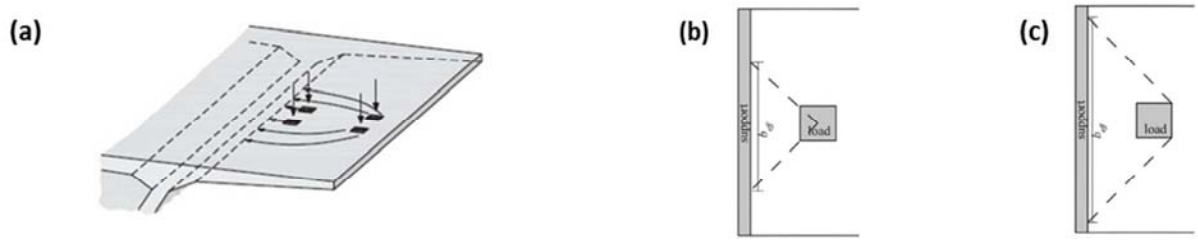


*Figure 1: Effective width evaluation for bridge deck slab subjected to concentrated loads linearly supported: (a) according to shear fields definition [6]; or assuming 45 – degree horizontal load spreading (b) from center of load; and (c) from far corners of load [3]*

shear forces after cracking or yielding of the reinforcement [6]. The present work will investigate the behaviour of RC slabs under concentrated loads close to linear supports by means of NLFE analyses and analytical procedures. The shear resistance of the specimens investigated has been evaluated firstly by means of the Critical Shear Crack Theory, CSCT, [7], considering the formulation for one – way slabs, then by means of multi – layered shell elements modelling and PARC_CL Crack Model [8], [9] associated to a post – processing Method, [10], [11].

## 2 Critical Shear Crack Theory (CSCT)

The Critical Shear Crack Theory allows determining the shear strength of slender one or two – way slabs on the basis of the opening of the critical shear crack [7]. This formulation points out that failure in shear occurs when the critical crack propagates through the inclined compression strut, limiting its strength and not allowing the member to reach the flexural capacity. Muttoni et al. [7] proposed a failure criterion in terms of one – way shear that estimates the maximum shear force for a given critical crack width. Such parameter can be assumed proportional to the product of a reference longitudinal strain $\varepsilon$ times the effective depth $d$. CSCT evaluates the shear strength in the critical section at *0.5d* from the point of maximum acting moment. The reference longitudinal strain is assessed at *0.6d* from the outer compressive fibre considering a linear elastic behavior for concrete in compression, neglecting concrete tensile strength (Figure 2). Hence, taking into account of the effects of the critical shear crack width, the aggregate size $d_g$ and the concrete compressive strength $f_c$, the failure criterion is described by Eq. (1):

$$v_c(\varepsilon) = \frac{d\sqrt{f_c}}{3}\frac{1}{1+\frac{120\varepsilon d}{16+d_g}} \quad (1)$$

The longitudinal strain $\varepsilon$ and the $c_{flex}$ are defined by Eq. (2) and (3):

$$\varepsilon = \frac{m}{d\rho E_s\left(d-\frac{c_{flex}}{3}\right)}\frac{0.6d-c_{flex}}{d-c_{flex}} \quad (2)$$

$$c_{flex} = d\rho\frac{E_s}{E_c}\left(\sqrt{1+\frac{2E_c}{\rho E_s}}-1\right) \quad (3)$$

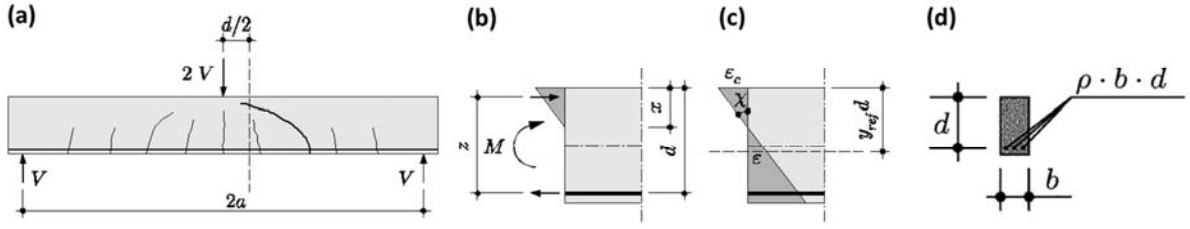


*Figure 2: (a) Critical section for point loading; (b) – (c) Evaluation of longitudinal strain in control depth 0.6d; (d) Definition of effective depth d and width b [7]*

# 3 Assessment methods of the shear resistance

## 3.1 Analytical formulation in accordance to CSCT

Experimental outcomes carried out by Natario et al. [6] show for linearly supported slabs under concentrated loads clear and rather significant redistributions of the reactions. Redistributions occur not only due to bending cracks but also for the development of the inclined shear crack. Indeed, as the level of applied load increases, the reaction in the region close to the load enhances at a slower rate because load starts to be transferred to the adjacent regions which are less affected by the shear crack. To account for this distribution of internal forces, an average shear stress $v_{avg,4d}$, is calculated along a distance 4d assuming unitary shear stresses obtained by LEFE analysis. The flowchart, illustrated in Figure 4 shows that the reference longitudinal strain $\varepsilon_i$ is calculated at the location of the maximum unitary acting moment $m_i$. Then, it is calculated the parameter *k,* as the ratio of the acting moment $m_i$ to the average unitary shear $v_{avg,4d}$ (both of them evaluated in the critical section). Hence, the ultimate shear failure value $V_R$ is evaluated following an iterative procedure, as it is shown in the flowchart of Figure 4, at the intersection with the failure criterion of Eq. (1).

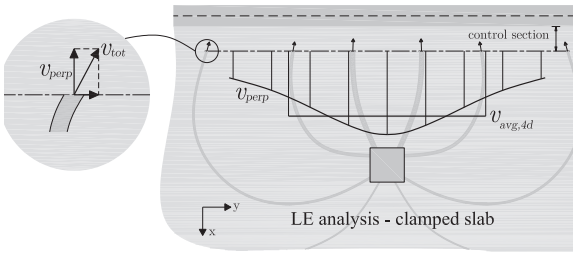


*Figure 3: Definition of the averaged shear force $v_{avg,4d}$ [6]*

In order to take into account of arching action that can occur in case of shear spans ranging from *2d* to *3d [6],* a factor β is applied to increase the shear resistance, according to Eq.(4):

$$V_R = \frac{v_{c,n}}{\beta} b \qquad (4)$$

Being b the length evaluated from LEFE analysis results as the ratio $F_{hypothesis}/v_{avg,4d}$.

The factor β is given by Eq. (5):

$$\beta = \frac{a_v}{2.75d} \leq 1 \qquad (5)$$

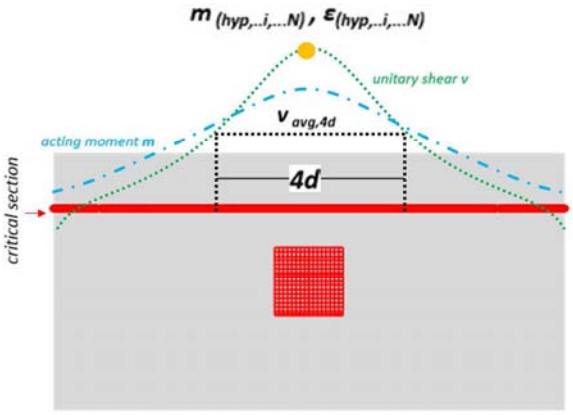


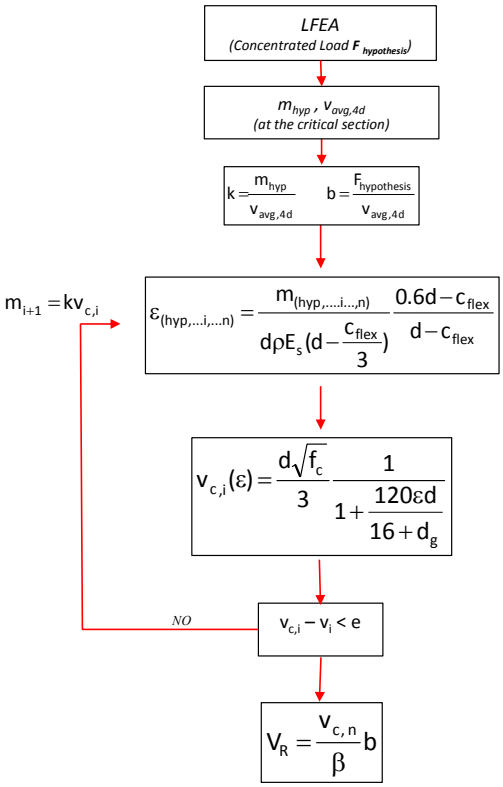


*Figure 4: Flowchart of the main steps for the evaluation of the shear resistance value in accordance to CSCT*

### 3.2 Multi – layered shell elements modelling

In the MC2010, LoA IV corresponds to the maximum level of detail and precision of evaluation. LoA IV encloses nonlinear analyses able to obtain very accurate results although complexity and numerical effort are quite high. For this research, NLFE analyses with PARC_CL Crack Model [8], [9] were carried out using multi – layered shell elements modelling. By adopting this kind of modelling, it is possible to divide the thickness in different layers in order to simulate correctly the reinforcement location along the thickness.

PARC_CL Crack Model [8], [9] is based on a fixed total strain crack approach. Two reference systems are defined at each integration point: the local x, y coordinate system and the 1, 2 coordinate system along the principal stress directions (Figure 5). The concrete behaviour is assumed to be orthotropic, both before and after cracking; softening in tension and compression, a multi – axial state of stress and aggregate interlock are taken into consideration. Reinforcement modelling consists in a smeared approach; dowel action and tension stiffening phenomena are taken into account. The overall stiffness matrix in the x,y coordinate system is evaluated considering that concrete and reinforcement behave like two springs placed in parallel.

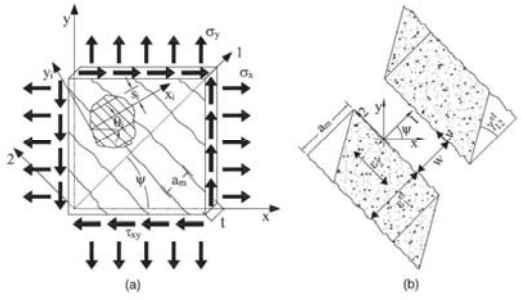


*Figure 5: (a) RC membrane elements subjected to plane stresses; (b) Kinematics quantities [8],[9]*

Multi – layered shell modelling associated with PARC_CL Crack Model estimates only plane stresses without considering the increase of deformability due to the opening of the critical shear crack. For this reason, out – of – plane shear failures cannot be detected with this kind of modelling. Consequently, the evaluation of shear resistance is achieved with a post – processing method by intersecting the Load – Strain curve obtained by the NLFE analyses with the failure criterion, described by Eq. (1) (refer to Figure 6).

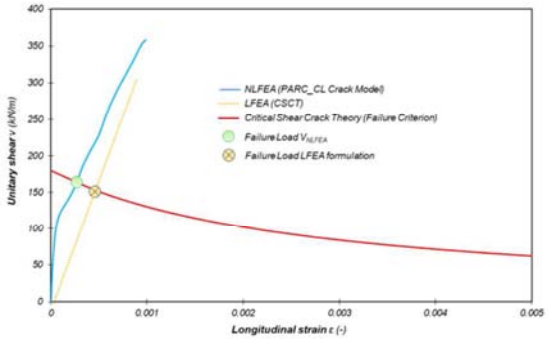


*Figure 6: Definition of the ultimate shear value (green circle) with the post – processing method*

## 4 Experimental programmes of Natario and Rombach et al.

The details of these two experimental campaigns can be found in publications by Natario et al. [6] and Rombach et al. [12]. The experimental setup and test results will be pointed out in the following section in order to compare them, firstly, to analytical formulations and, consequently, to assessments by means of NLFE analyses with PARC_CL Crack Model [8].

### 4.1 Campaign of Natario

#### 4.1.1 Test setup

Twelve tests were performed on six RC square slabs (3000 x 3000 x 180 mm) at the Ecole Polytechnique Fédérale de Lausanne. All the slabs have a 180 mm nominal thickness with a thickening at the gusset in the central region (280 mm). The flexural nominal depth *d* is 152 mm for each specimen. Three tests have been performed on slabs without ducts, three on slabs with empty ducts, three on slabs with injected steel ducts and three on injected polypropylene ducts (cross sections in Figure 9) to simulate a situation which typically occurs in bridges designed with the free cantilever method (where longitudinal tendons are placed in the deck slab). Each slab is centrally

supported by means of an I –shaped aluminium profile equipped with strain gauges to measure the distribution of reactions. The loading arrangement consists in two hydraulic actuators with a concentrated load distant $a_v$ from the end of the gusset. Figure 8.a shows schematically the test setup while Figure 8.b exhibits the reinforcement layout of top and bottom layer. For the main mechanical properties of the materials, refer to [6].

### 4.1.2 Observations on the experimental results

At the top surface of each slab, the cracking pattern developed almost parallel to the linear support in the central region while for the bottom surface, cracking developed more or less perpendicular to the linear support and concentrated near the loading area (Figure 7). The observations on the critical shear crack exhibits that cracks developed from a flexural crack at a certain distance from the loading plate and the shear crack is not located at the tip of loading plate (as in punching shear failures). For this reason, the failure might be analysed in terms of a one – way shear. Table 2 shows the maximum loads for all tests: it can be noticed that there is a reduction of the shear strength due to an increase of the ratio $a_v/d$ where $a_v$ is the shear span. These results denote a significant influence of the arching action but, also, a potential influence of the bending moments on the shear resistance.

### 4.1.1 Multi – layered shell element modelling

All specimens were modelled with eight shell elements (*SR8*). Shell element thickness was divided into three layers in order to consider top and bottom steel reinforcement. Only a quarter of slab (Figure 10) was modelled in order to consider symmetrical conditions along *x* and *y* directions. The loading system was modelled as a region in which a constant pressure was applied. The aluminium profile was simulated by means of nonlinear spring elements that work only in compression with a very low stiffness in tension.

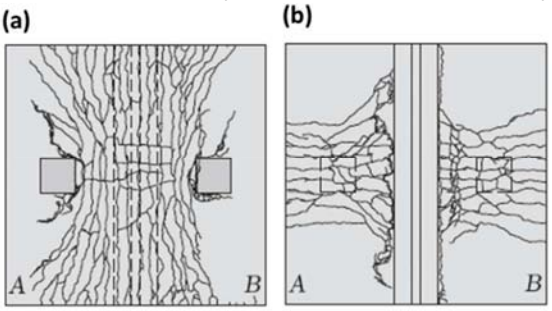


*Figure 7: Cracking pattern after failure for SN2: (a) top face; (b) bottom face [6].*

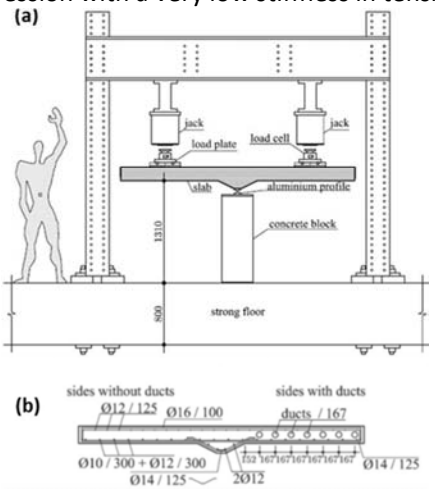


*Figure 8: (a) Test setup for Natario's experimental program; (b) Reinforcement layout (in mm), [6]*

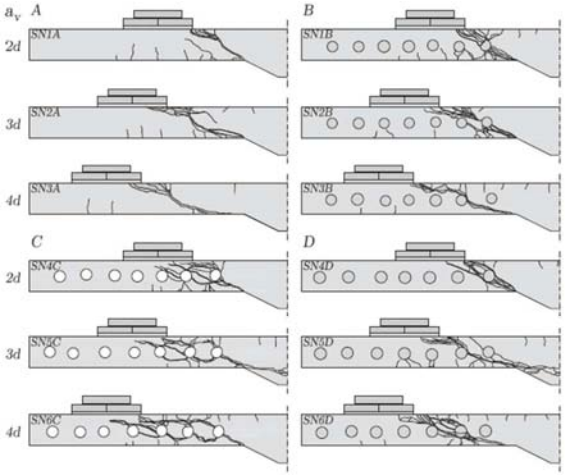


*Figure 9: Cross – sections of the specimens [6]*

*Figure 10: Shell modelling of a quarter slab*

## 4.2 Campaign of Rombach et al.

### 4.2.1 Test setup

The experimental campaign consisted in twelve tests on four full – scale specimens of RC deck slabs. Geometrically, each slab is 2.4 m in width, ranging from 5.68 m to 6.58 m in length. Two specimens had a constant thickness, respectively, of 250 mm and 200 mm while the other ones were tapered slabs with variable thickness. Each test specimen consists in two cantilever slabs of 1.65 m span and a central slab supported by two web beams. Hence, two cantilever tests (V1 and V2) and a centre slab test (V3) have been carried out for each specimen. We will discuss only about the cantilever tests, focusing on those ones without shear reinforcement (V1). As regards loading, a constant line load $f_q$ has been applied over the full width of the cantilever tests. In a second step, a point load $F_Q$ has been enforced on a square loading plate until failure. Figure 11 describes the test setup and load arrangement. For the main mechanical properties of the materials, refer to [12].

### 4.2.1 Discussion of the experimental results

The cantilever deck slabs without shear reinforcement (V1) failed in a brittle manner before the onset of rebar yielding. As regards the cracking pattern of tests *V1* (Figure 12), on the top surface of each slab, cracks developed almost parallel to the support while for bottom surface, cracking was mostly concentrated close to the loading area, perpendicularly to the linear support.

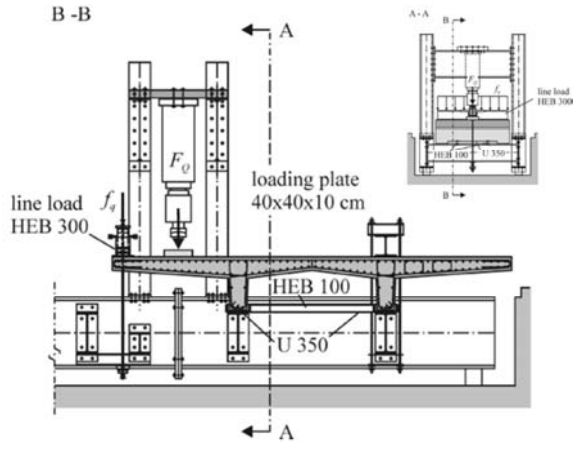


*Figure 11: Test setup and load arrangement of the cantilever tests [12]*

### 4.2.2 Multi – layered shell element modelling

As previously mentioned, all specimens were modelled with eight nodes shell elements (*SR8*). For the tapered slab (Figure 13), the variation of thickness was modelled in order to approximate as much as possible the real geometrical properties of the specimens. Both linear load $f_q$ and concentrated load $F_Q$ were modelled considering a region in which a constant pressure was applied. In order to have a good agreement with the test setup, the supporting beams were modelled in their middle plane. Such supporting systems were fixed preventing the slab to lift up.

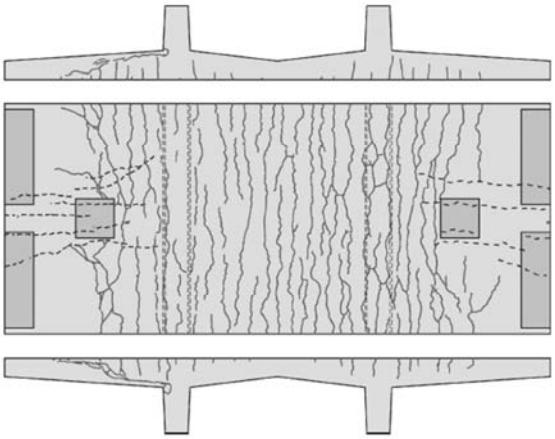

*Figure 12: Cracking pattern after test V1 without shear reinforcement (left cantilever) and test V2 (right cantilever), [12]*

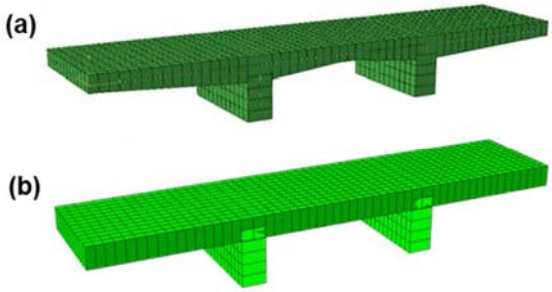


*Figure 13: Shell modelling in case of: (a) variable thickness; and (b) constant thickness*

## 5 Discussion and comparison of the results

Table 1 and Table 2 show a comparison between test results and predictions by means of LFEA formulation according to CSCT and numerical outcomes with PARC_CL Crack Model [8], [9] associated to the post –processing Method. In Tables 1 and 2, $V_{NLFEA,failure}$ represents the ultimate shear resistance value by intersecting the unitary shear – longitudinal strain curve obtained with NLFEA and the failure criterion according to CSCT. Arching action is taken into account for specimens with shear span $a_v$ less than 2.75d according to Eq. (4). The comparisons of Table 1 and Table 2 point out how numerical results of PARC_CL Crack Model post – processed in accordance to CSCT, are able to predict in the right way the trends and measured shear strength. The average value of the ratio between the experimental and calculated strength are closer to 1.0 with low values of the Coefficient of Variation COV. Nevertheless, the assumption of an averaged shear force $v_{avg,4d}$ should be analysed very carefully. As we can see in the shear fields of Figure 14, the development of shear forces for specimen SN2A is quite different from specimen VK3 characterized by an uniform distribution along the entire width of the slab, very similar to one way slab shear mechanism.

*Table 1: Comparison between tests and shear strength predictions (Latte)*

| Test | $V_{exp}$ [kN] | $V_{NLFEA,failure}$ [kN] | $\frac{V_{exp}}{V_{NLFEA,failure}}$ | LFEA formulation (CSCT) |
|---|---|---|---|---|
| **VK1** V1 | 690 | 599.1 | 1.15 | 1.36 |
| **VK2** V1 | 678 | 583.0 | 1.16 | 1.52 |
| **VK3** V1 | 672 | 667.0 | 1.01 | 1.33 |
| **VK4** V1 | 487 | 355.9 | 1.37 | 1.51 |
| **COV** | | | 0.13 | 0.07 |
| **AVG** | | | 1.17 | 1.43 |

*Table 2: Comparison between tests and shear strength predictions (Natario)*

| Test | $V_{exp}$ [kN] | $V_{NLFEA,failure}$ [kN] | $\frac{V_{exp}}{V_{NLFEA,failure}}$ | LFEA formulation (CSCT) |
|---|---|---|---|---|
| **SN1A** | 489 | 466.6 | 1.05 | 1.22 |
| **SN2A** | 330 | 336.0 | 0.98 | 1.05 |
| **SN3A** | 328 | 343.2 | 0.96 | 1.03 |
| **SN1B** | 437 | 452.7 | 0.97 | 1.12 |
| **SN2B** | 341 | 333.3 | 1.02 | 1.10 |
| **SN3B** | 330 | 340.4 | 0.97 | 1.05 |
| **SN4C** | 307 | 325.2 | 0.94 | - |
| **SN5C** | 266 | 250.2 | 1.06 | - |
| **SN6C** | 234 | 252.3 | 0.93 | - |
| **SN4D** | 494 | 457.9 | 1.08 | 1.26 |
| **SN5D** | 335 | 329.8 | 1.02 | 1.09 |
| **SN6D** | 327 | 337.3 | 0.97 | 1.05 |
| **COV** | | | 0.05 | 0.07 |
| **AVG** | | | 1.00 | 1.11 |

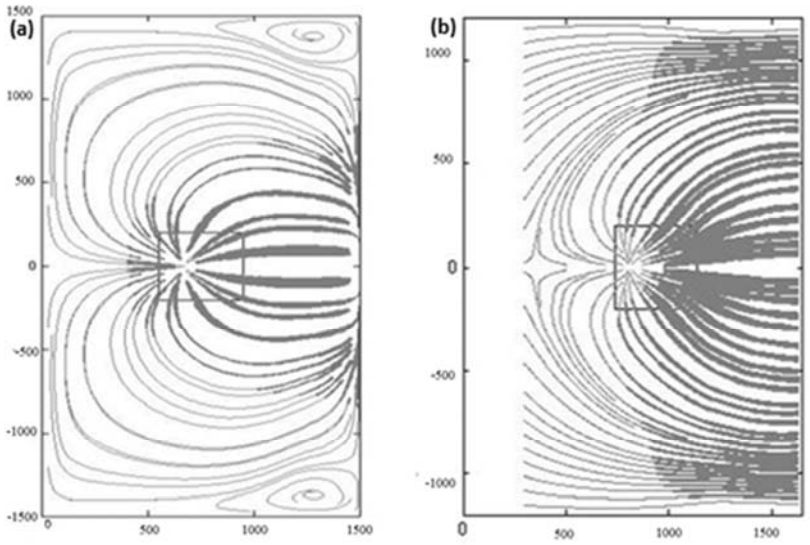


*Figure 14: Comparison of the shear fields for: (a) SN2A; and (b) VK3*

## 6 Conclusions

This work investigates the analytical and numerical predictions of ultimate shear strength for bridge deck slabs subjected to point loading.

The main conclusions of this paper are:

1. Multi –layered shell element modelling with PARC_CL Crack Model associated to the post – processing method according to CSCT gives consistent results in the evaluation of the shear resistance of the experimental programmes investigated.
2. The choice of assuming an average value of the unitary shear stresses on a certain width [6] calibrated experimentally may be not suitable for generic cases in which boundary and loading conditions could influence the distribution of shear stresses (Figure 14).
3. Since the ratio of bending moments to shear force for slabs under concentrated loads considerably varies from that of beams, the real boundary conditions of bridge deck slabs should be modelled properly for a correct evaluation of the shear strength.
4. Further researches should focus on how to apply the knowledge gathered from the experiments to more advanced numerical assessment procedure.

## 7 References

[1] Rombach G., Kohl M., Shear design of RC bridge deck slabs according to Eurocode 2, *J. Bridge Eng.* 2013;**18**:1261 – 9

[2] Vaz Rodrigues R. Shear strength of Reinforced Concrete bridge deck slabs. PhD Thesis, EPFL, Lausanne, 2007

[3] Lantsoght E. van der Veen C., de Boer A. and Walraven J.C. Influence of width on shear capacity of Reinforced Concrete Members. *ACI Structural Journal*, 2014. **111**: 1441 – 1450

[4] Lantsoght E., Van der Veen C., Walraven J.C., Shear in one – way slabs under concentrated load close to support. *ACI Structural Journal*. 2013; **110**(2): 275 – 84

[5] Lantsoght E., Van der Veen C., de Boer A. and Walraven J.C. Proposal for the extension of the Eurocode shear formula for one – way slabs under concentrated loads. *Engineering Structures*. 2015; **95**: 16 – 24

[6] Natario F., Muttoni A. and Fernàndez Ruiz M. Shear strength of RC slabs under concentrated loads near clamped linear supports, *Engineering Structures*. 2014; **76**: 10 – 23

[7] Muttoni A. and Fernàndez Ruiz M. Shear strength of members without transverse reinforcement as function of critical shear crack width, *ACI Structural Journal*. 2008; **105**(2):163 – 72

[8] Belletti B., Cerioni R. and Iori I Physical Approach for Reinforced-Concrete (PARC) membrane elements. *ASCE Journal of Structural Engineering*. 2001; **127**: 1412-1426

[9] Belletti B, Esposito R. and Walraven J.C. Shear Capacity of Normal, Lightweight, and High-Strength Concrete Beams according to Model – Code 2010. II: Experimental Results versus Nonlinear Finite Element Program Results. *Journal of Structural Engineering.* 2013; **139**:1600 – 1607

[10] Belletti B., Damoni C., Max A. N. Hendriks and de Boer A. Analytical and numerical evaluation of the design shear resistance of reinforced concrete slabs. *Structural Concrete*. 2013; **139**:1593 – 1599

[11] Belletti B. Walraven J.C., Trapani, F. Evaluation of compressive membrane action effects on punching shear resistance of reinforced concrete slabs. *Engineering Structures*. 2015; **95**: 25-39

[12] Rombach G. and Latte S. Shear resistance of bridge decks without transverse reinforcement. *Beton Stahlbetonbau*. 2009; **104**(10):642 – 56 [in German]